Yuta Yamada, JGRG 22(2012)111337

"Numerical study of 5-dimensional gravitational collapses"

RESCEU SYMPOSIUM ON

GENERAL RELATIVITY AND GRAVITATION

JGRG 22

November 12-16 2012

Koshiba Hall, The University of Tokyo, Hongo, Tokyo, Japan

Numerical Study of Five-dimensional Gravitational Collapses

[(a)]Yuta Yamada[1] and [(a),(b)]Hisa-aki Shinkai[2]

[(a)] *Faculty of Information Science and Technology, Osaka Institute of Technology, Hirakata, Osaka 573-0196, Japan*
[(b)] *Computational Astrophysics Laboratory, Institute of Physical & Chemical Research (RIKEN), Hirosawa, Wako, Saitama 351-0198, Japan*

Abstract

Five-dimensional black-hole and black-ring formation are investigated numerically. We model the initial matter distribution in homogeneous spheroidal and toroidal configurations under the momentarily static assumption and express the matter with collisionless particles. Evolutions of space-time and particles are followed by using ADM formalism ($4+1$ decomposition) and solving the geodesic equation. For spheroidal configurations, we repeat the simulation performed by Shapiro and Teukolsky (1991) that announced an appearance of a naked singularity, and also find similar results in the 5D version. For toroidal configurations in U(1)× U(1) symmetry, we consider the rotating collisionless particles which consist of equal numbers co-rotating and counter-rotating under a certain rotational law. We search both spherical(S^3) and ring-shaped($S^2 \times S^1$) horizons, and show topology change of apparent horizon from ring-shaped to spherical shape during its evolution. We also discuss whether an observer at the origin of the ring-horizon can escape out or not.

1 Introduction

For a decade, higher-dimensional black-holes are extensively studied linked with the so-called "large extra-dimensional models". The discovery of black-ring solution[1] with horizon of $S^2 \times S^1$ topology in U(1)× U(1) space, and its associated Saturn-type "black objects" reveal new features of higher-dimensional space-time. However, non-linear dynamical features, such as formation process, generality, and stability of black-objects, are not yet known. We plan to investigate these outstanding problems using numerical simulations. In this article, we report two models.

First topic is on the naked singularity formation. Shapiro and Teukolsky[2] (ST91) numerically showed that in four-dimensional(4D) space-time, collisionless matter particles in spheroidal distribution will collapse to singularity, without forming apparent horizon(AH) when the spheroids are highly prolate. We report their simulations and compare them with those in 5D(§3)[3].

Second topic is the formation of black-ring in 5D(§4). We distributed collisionless matter particles in toroidal configuration, and evolve them with/without their rotations. As the first step, we assume particles are counter-rotating and the system's net angular momentum is zero. We search both AH of spherical and ring-shaped during time evolution.

2 Our numerical code

For the simulation of spheroidal collapses, we evolve five-dimensional axisymmetric [symmetric on z-axis, SO(3)] or doubly-axisymmetric [symmetric both on x and z-axes, U(1)×U(1)], asymptotically flat space-time (see Figure 1). For the comparison, we also performed four-dimensional axisymmetric space-time evolutions.

We start our simulation from time symmetric and conformally flat initial data, which are obtained by solving the Hamiltonian constraint equations [4]. The asymptotical flatness is imposed throughout

[1]Email address: yamada@is.oit.ac.jp
[2]Email address: shinkai@is.oit.ac.jp

the evolution, which settles the fall-off condition to the metric as $\sim 1/r$ for 4D cases and $\sim 1/r^2$ for 5D cases.

The matter is described with 5000 collisionless particles, which move along the geodesic equations. We smooth out the matter by expressing each particle with Gaussian density distribution function with its typical width is twice as much as the numerical grid. The particles are homogeneously distributed in a spheroidal shape, parametrized with a and b (Figure 1), or eccentricity $e = \sqrt{1 - a^2/b^2}$.

By imposing axisymmetry or double-axisymmetry, our model becomes practically a (2+1)-dimensional problem. We construct our numerical grids with the Cartesian coordinate (x, z), and apply the so-called Cartoon method [5] to recover the symmetry of space-time.

The space-time is evolved using the Arnowitt-Deser-Misner (ADM) evolution equations. It is known that the ADM evolution equations excite an unstable mode (constraint-violation mode) in long-term simulations [6, 7]. However, we are free from this problem since gravitational collapse occurs within quite short time. By monitoring the violation of constraint equations during evolutions, we confirm that our numerical code has second-order convergence, and also that the simulation continues in stable manner. The results shown in this report are obtained with numerical grids, 129×129×2×2. We confirmed that higher resolution runs do not change the physical results.

We use the maximal slicing condition for the lapse function α, and the minimal strain condition for the shift vectors β^i. Both conditions are proposed for avoiding the singularity in numerical evolutions [8], and the behavior of α and β^i roughly indicates the strength of gravity, conversely. The iterative Crank-Nicholson method is used for integrating ADM evolution equations, and the Runge-Kutta method is used for matter evolution equations.

For discussing physics, we search the location of apparent horizon (AH), calculate the Kretschmann invariant ($\mathcal{I} = R_{abcd}R^{abcd}$) on the spacial hypersurface.

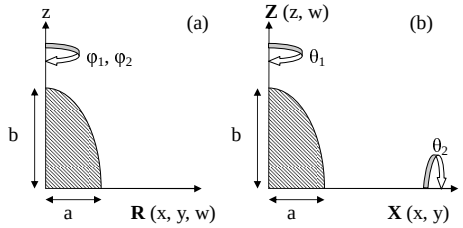

Figure 1: We evolve five-dimensional (a) axisymmetric [SO(3)] or (b) double-axisymmetric [U(1)× U(1)], asymptotically flat space-time using the Cartesian grid. The initial matter configuration is expressed with parameters a and b.

For the simulation of toroidal collapses, we evolve doubly-axisymmetric [symmetric both on x and z-axes, U(1)×U(1)], asymptotically flat space-time (see Figure 2). We use the maximal slicing condition for the lapse function α, and the zero shift condition for the shift vectors β^i.

In this paper, we consider the toroidal configuration which consist of equal number corotating and counter-rotating particles under the Kepler like law $V(r) \propto \xi/r$ where ξ is the arbitrary rotational parameter. Although each particles move on the x-z section, there are no net angular momentum. Hence we only solve the Hamiltonian constraint equation for preparing the initial data.

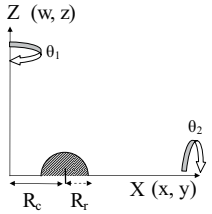

Figure 2: We evolve double-axisymmetric [U(1)× U(1)], asymptotically flat space-time using the Cartesian grid. The initial matter configuration is expressed with parameters R_c and R_r.

3 Results of spheroidal collapses

We prepare several initial data keeping the total ADM mass and the eccentricity of distribution, $e = 0.9$. By changing the initial matter distribution sizes, we observe the different final structures. Figure 3 shows snapshots of 5D axisymmetric evolutions of model $b/M = 4$ and 10 (model 5DSβ and 5DSδ, respectively; see Table 1); the former collapses to a black hole while the latter collapses without AH formation.

b/M $(t = 0)$	2.50	4.00	6.25	10.00
4D axisym.	4Dα	4Dβ	4Dγ	4Dδ
	AH-formed	no	no	no
	$e_{\rm AH} = 0.90$			
	$e_{\rm f} = 0.92$	$e_{\rm f} = 0.89$	$e_{\rm f} = 0.92$	$e_{\rm f} = 0.96$
5D axisym. SO(3)	5DSα	5DSβ	5DSγ	5DSδ
	AH-formed	AH-formed	no	no
	$e_{\rm AH} = 0.88$	$e_{\rm AH} = 0.88$		
	$e_{\rm f} = 0.82$	$e_{\rm f} = 0.84$	$e_{\rm f} = 0.88$	$e_{\rm f} = 0.96$
5D double axisym. U(1)×U(1)	5DUα	5DUβ	5DUγ	5DUδ
	AH-formed	AH-formed	AH-formed	no
	$e_{\rm AH} = 0.86$	$e_{\rm AH} = 0.87$	$e_{\rm AH} = 0.92$	
	$e_{\rm f} = 0.79$	$e_{\rm f} = 0.81$	$e_{\rm f} = 0.90$	$e_{\rm f} = 0.98$

Table 1: (above) Model-names and the results of their evolutions whether we observed AH or not. The eccentricity e the collapsed matter configurations is also shown; $e_{\rm AH}$ and $e_{\rm f}$ are at the time of AH formed (if formed), and on the numerically obtained final hypersurface, respectively.

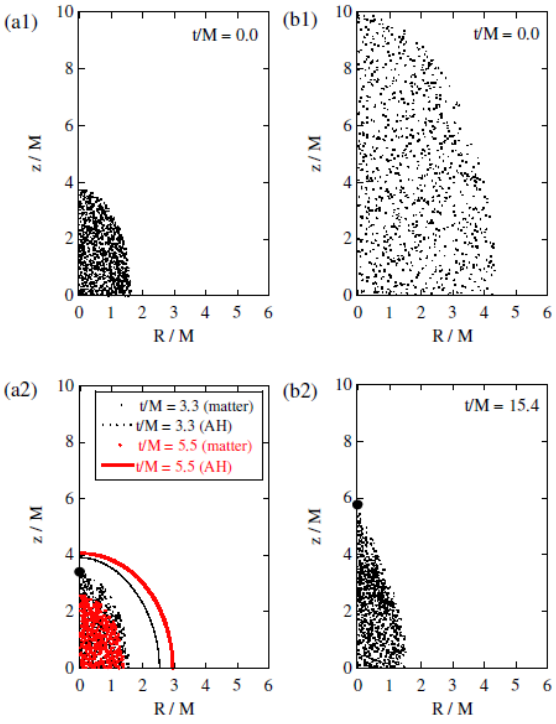

Figure 3: (right) Snapshots of 5D axisymmetric evolution with the initial matter distribution of $b/M = 4$ [Fig.(a1) and (a2); model 5DSβ in Table 1] and 10 [Fig.(b1) and (b2); model 5DSδ]. The big circle indicates the location of the maximum Kretschmann invariant $\mathcal{I}_{\rm max}$ at the final time at each evolution.

All the models we tried result in forming a singularity (i.e., diverging $\mathcal{I}$). We stop our numerical evolutions when the shift vector is not obtained with sufficient accuracy due to the large curvature. For model 5DSδ, we integrated up to the coordinate time $t/M = 15.4$ and the maximum of the Kretschmann invariant $\mathcal{I}_{\rm max}$ becomes $O(1000)$ on z-axis (see Figure 3), but AH is not formed.

When the initial matter is highly prolated, AH is not observed. This is consistent with 4D cases [2], and matches with the predictions from initial data analysis in 5D cases [4, 9]. The location of $\mathcal{I}_{\rm max}$ is on z-axis, and just outside of the matter. This is again the same with 4D cases [2]. The absence of AH with diverging $\mathcal{I}$ suggests a formation of naked singularity in 5D.

In order to compare the results with 4D and 5D, we reproduce the results of ST91. We then find that the $e = 0.9$ initial data with $b/M = 10$ (model 4Dδ) collapses without forming AH, and the code stops at the coordinate time $t = 20.91$ with $\mathcal{I}_{\rm max} = 84.3$ on the z-axis ($z/M = 6.1$); all the numbers match quite well with ST91. (Note that our slicing conditions and coordinate structure is not the same with ST91.)

We also performed 5D collapses with doubly-axisymmetric [U(1)×U(1)] space-time. The matter and space-time evolve quite similar to 5D and 4D axisymmetric cases, but we find that the critical configurations for forming AH is different. Table 1 summarizes the main results of 4D and two 5D cases. We find that AH in 5D is formed in larger b initial data than 4D cases. This result is consistent with our prediction from the sequence of initial data [4]. AH criteria with initial b is loosened for 5D doubly-axisymmetric cases. We show the eccentricity, $e_{\rm AH}$ and $e_{\rm f}$, which tell us that the doubly-axisymmetric assumption makes collapse less sharp when it forms AH, and makes collapse similar to 4D cases when it does not form AH. Table 1 indicates that the eccentricity itself is not a guiding measure for AH formation.

In Figure 4, we plotted $\mathcal{I}$ at the point which gives $\mathcal{I}_{\rm max}$ on the final hypersurface as a function of proper time. We see that 5D-collapse is proceeding rapidly than 4D collapses. We also see that collapses in doubly-axisymmetric space-time is proceeding slowly than single axisymmetric cases.

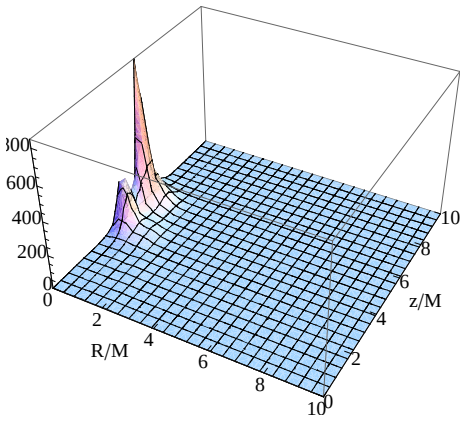

Figure 4: Kretschmann invariant $\mathcal{I}$ for model 5DSδ at $t/M = 15.4$. The maximum is $O(1000)$, and its location is on z-axis, just outside of the matter.

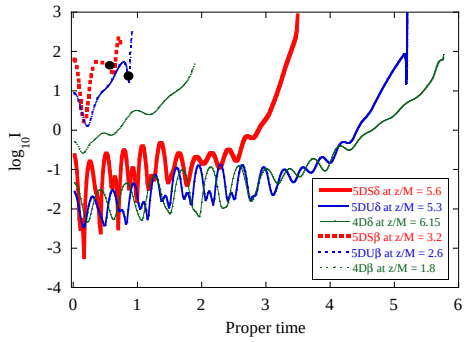

Figure 5: Kretschmann invariant $\mathcal{I}$ at the location of $\mathcal{I}_{\max}$ on the final hypersurface is plotted as a function of proper time at its location. labels indicate model-names in table 1. the time of ah formation (t=0.6 for model 5DSβ, t=0.9 for 5DUβ) is shown by a dot.

4 Results of toroidal matter collapses

Figure 6 shows that snapshots of evolutions of the non-rotating toroidal matter of which initial radius are (a) $R_c/r_s = 0.6$ and (b) 0.8, respectively. We observe a formation of spheroidal AH (common horizon) in upper panels, while we see a formation of toroidal AH (ring horizon) in a moment then it switches to common horizon in lower panels. Figure 7 shows the area of AHs as a function of coordinate time. Red and blue lines show the AH area during time evolutions of non-rotating and counter-rotating particles, respectively. We find that the area of horizon increases gradually during time evolution. We also find that for rotating-cases the appearance of AH delays and the area of horizon is smaller comparing to the non-rotating cases. These behavior are thought to be due to the delay of collapse by rotation effect. Furthermore, we show a numerical solution that the area of ring AH stays constant during time evolution (panel (b) in Fig.7). For the case of initial ring radius $R_c/r_s = 0.8$, AH is not formed during time evolution when parameter ξ is $\xi \geq 0.5$(the ratio of rotating energy to the total energy, $T/W = 0.19$). While for the case of initial ring radius $R_c/r_s = 1.5$, AH is not formed during time evolution when parameter ξ is greater than $0.2(T/W = 0.07)$.

For the case of $R_c(t = 0) = 0.8r_s$ and $\xi = 0$ (panel (a) in Fig.7), we check whether the observer at the origin who observed the appearance of the ring AH can escape outside or not. Fig.8 shows the snapshots of the hypersurfaces on x and z axis with the proper-time. In Fig.8, solid lines colored by red, blue and orange express a ring AH and common AH and light ray, respectively. For this case, the light ray which emitted from the inner ring AH reaches to the origin at proper-time $t = 0.75$ (left panel in Fig.8). Even if the observer tries to escape with the speed of light along to the Z-axis just after that time, he/she can not move outside of the common AH. We obtained the same result for the case of $R_c(t = 0) = 0.8r_s$ and $\xi = 0.3(T/W = 0.01)$. Our results indicate that when AH topology changes from ring-shaped to spherical, the observer cannot escape from these region. On the other hand, for the case of $R_c(t = 0) = 1.5r_s$ and $\xi = 0.1(T/W = 0.05)$ (panel (b) in Fig.7), as shown in Fig.9, the observer can escape from these region because of common AH is not formed.

5 Summary

In this article, we reported gravitational collapses of non-rotating spheroidal configurations, and non-rotating/counter-rotating toroidal configurations in 5D space-time. For time evolution of spheroidal configurations, we found the possibility of naked singularity formation. For time evolution of toroidal configurations, we see the formation of AH, and always we also found that topological transition of AH during the ring matter collapses where we observed monotonically increases of the area of AHs both

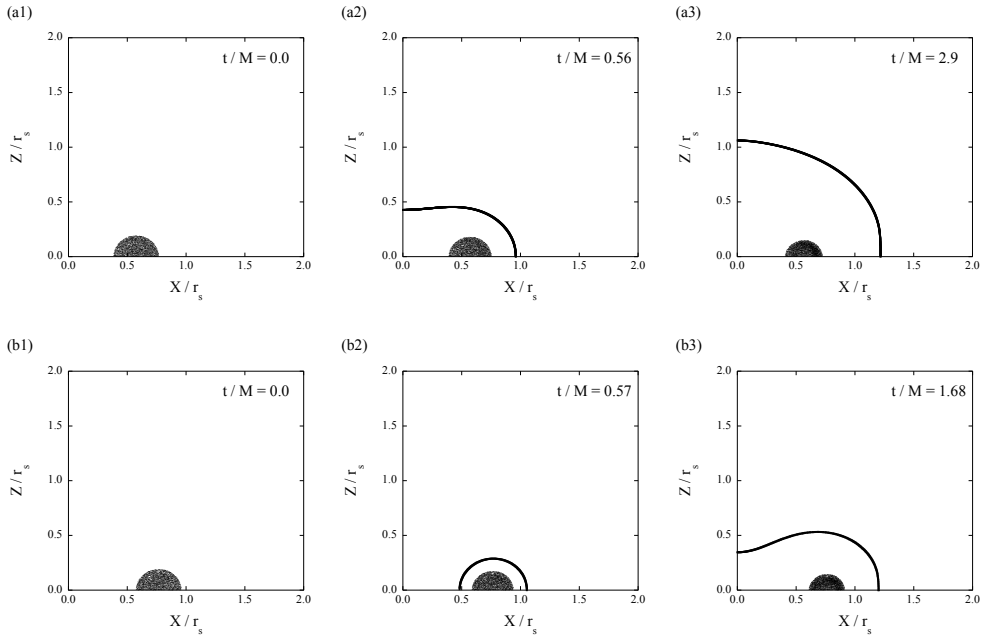

Figure 6: Snapshots of time evolutions, plotting particles and locations of AHs. We set initial ring radius $R_c/r_s = 0.6$ (upper panels), $R_c/r_s = 0.8$ (lower panels) and rotation parameter $\xi = 0$. We see that a common AH is directly formed at $t/M = 0.56$ in the panel (a2), while we see a topological transition of AHs from ring-shape to spherical at $t/M = 1.68$ in the panel (b3).

common and ring AHs.

Up to this moment, we only checked the existence of apparent horizons, and not the event horizons. The system does not include any net angular momentum. We are implementing our code to cover these studies.

This work was supported partially by the Grant-in-Aid for Scientific Research Fund of Japan Society of the Promotion of Science, No. 22540293. Numerical computations were carried out on SR16000 at YITP in Kyoto University, and on the RIKEN Integrated Cluster of Clusters (RICC).

References

[1] R. Emparan and H. S. Reall, Phys. Rev. Lett. **88**, 101101 (2002).

[2] S. L. Shapiro and S. A. Teukolsky, Phys. Rev. Lett. **66**, 994 (1991).

[3] Y. Yamada and H. Shinkai, Phys. Rev. D **83**, 064006 (2011).

[4] Y. Yamada and H. Shinkai, Class. Quant. Grav. **27**, 045012 (2010).

[5] M. Alcubierre, et al., Int. J. Mod. Phys. D**10**, 273 (2001).

[6] see e.g., H. Shinkai, J. Korean Phys. Soc. **54** 2513 (2009).

[7] H. Shinkai and G. Yoneda, Gen. Rel. Grav. **36** 1931 (2004).

[8] L. Smarr and J. W. York, Jr., Phys. Rev. D **17**, 2529 (1978).

[9] C-M. Yoo, K. Nakao and D. Ida, Phys. Rev. D **71**, 104014 (2005).

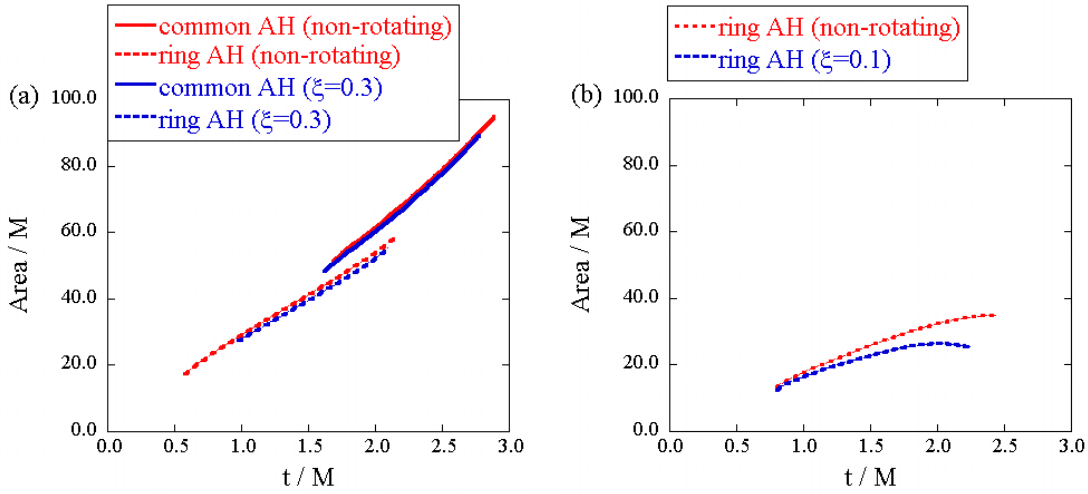

Figure 7: Area of AHs of both common and ring-shaped. The panels (a) and (b) show the results of time evolution for initial ring radius $R_c/r_s = 0.8$ and 1.5, respectively. Red and blue lines show AHs area during time evolution of non-rotating and counter-rotating particles, respectively. We see that the area of horizon increase gradually during time evolution. We also find that for rotating-cases the appearance of AH delays and the area of horizon is smaller comparing to the non-rotating cases.

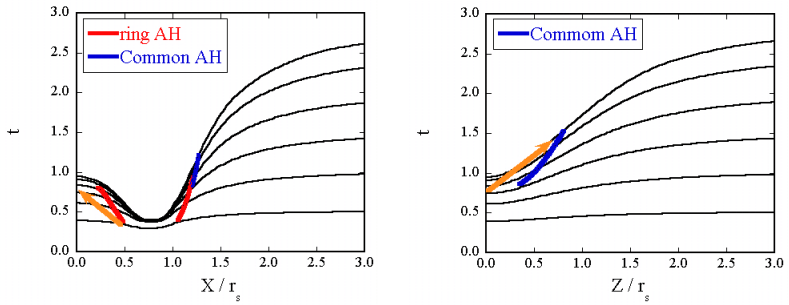

Figure 8: The snapshots of the hypersurfaces on x and z axis in the proper-time τ. The arrow indicates the path of light starting from the appearance of the ring horizon (left panel), and starting from the moment of such information arrives on the Z-axis. The arrow hits the common AH on Z-axis, which indicates the observer at the origin cannot escape if he/she observes the appearance of a ring-shaped horizon.

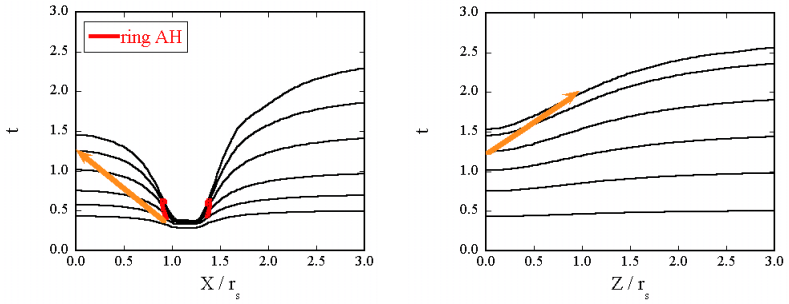

Figure 9: The same with Fig.8 for the case of $R_c(t=0) = 1.5r_s$ and $\xi = 0.1(T/W = 0.05)$. This case shows the observer at the origin can escape even if he/she observes the appearance of a ring-shaped horizon, since the common AH is not formed.